Contents lists available at ScienceDirect

Journal of Network and Computer Applications

journal homepage: www.elsevier.com/locate/jnca

Reactive power control for an energy storage system: A real implementation in a Micro-Grid

D.A. Sbordone [a,*], L. Martirano [a], M.C. Falvo [a], L. Chiavaroli [a], B. Di Pietra [b], I. Bertini [b], A. Genovese [b]

[a] DIAEE - Electrical Engineering, University of Rome Sapienza, via Eudossiana 18, 00184 Rome, Italy

[b] ENEA, Italian National Agency for New Technologies, Energy and Sustainable Economic Development, Via Anguillarese 301, 00123 Roma, Italy

ARTICLE INFO

Keywords:
Charging stations
Energy storage
Information and communication technologies
Smart Grid
Micro-Grid
Smart metering

ABSTRACT

In last years, the power system operators are tackling many challenges for the renewable energies integration on the grid. Further, the expected increase of electrical demand due to the uncoordinated contemporary charging of a huge number of Electric Vehicles (EVs) can create chaotic phenomena with a negative impact especially on the distribution network. Help can be offered by the deployment of Smart Grid technologies, such as Smart Metering Systems (SMSs), Information and Communications Technology (ICT) and Energy Storage Systems (ESSs). In particular, in Micro-Grids, Battery ESSs (BESSs) can play a fundamental role and can become fundamental for the integration of EV fast charging stations and distributed generations. In this case the storage can have peak shaving, load shifting and power quality functions. The ESSs can provide ancillary services also on the grid as the reactive control to adjust the power factor. In the present paper, a monitoring control program to manage the reactive power of a real ESS in a Micro-Grid has been implemented. The system is a prototype, designed, implemented and now available at ENEA (Italian National Agency for New Technologies, Energy and Sustainable Economic Development) labs. A wide experimental activity has been performed on the prototype system in order to test this functionality for the integration in a bigger Smart Grid available at the same ENEA labs including the Micro-grid. The integration has been possible, thanks to the free ICT protocols used by the researchers and which are described here. The results of the experimental tests show that the system can have good performance to adjust the power factor in respect to the main distribution grid and an EV charging station.

1. Introduction

A Smart Grid is commonly defined as a portion of an MV/LV distribution network, assembled and operated by the Distribution System Operator (DSO) with the help of ICT, in order to improve the efficiency, reliability, economics, and sustainability of the production and distribution of electricity (Jackson 2014). The typical scale of a Smart Grid can be considered as a portion of an MV system supplied by an HV/MV substation.

A Micro-Grid is commonly defined as a group of interconnected loads and Distributed Energy Resources (DER) with clearly defined electrical boundaries that acts as a single controllable entity with respect to the main grid. In other words it is a smaller portion of the network, typically supplied by an MV/LV substation operated by a private user (or even by an aggregator) with the help of ICT (Tao et al., 2011). Typically, Smart Grids and Micro-Grids contain Distributed Generation (DG), Smart Metering Systems (SMSs) and an ICT infrastructure (Skopik et al., 2014; Falvo et al., 2013; Arboleya et al., 2015). The differences between Smart Grid and Micro-Grid are not only in terms of energy scale and voltage level but also in terms of goal of the operation (Huang et al., 2014). A Smart Grid operates in order to resolve the power unbalancing issues and other technical problems in real time and the DSO, that is, its player could offer new energy services to the users. A Micro-Grid operates in order to optimize the energy fluxes and, mostly, the energy costs and the user (or the aggregator), that is, the player could offer new services to the DSO (López et al., 2015). So, the distribution networks are strongly going to change their infrastructure allowing high penetration of DG such as wind power plants, photovoltaic plants and cogeneration units. Further, the EVs will spread more and more (Ustun et al., 2013; Pillai et al., 2012). So, due to partial unpredictability of both load and power generation from some renewable sources, power unbalances occur between the generation and the load on the grid. The DSOs are developing Smart Grid examples to supply intelligence to the grid through SMSs and an ICT infrastructure. Main capabilities of the Smart Grid system include the integration and aggregation of distributed

* Corresponding author. Tel.: +39 3402818606.
E-mail address: danilo.sbordone@uniroma1.it (D.A. Sbordone).

http://dx.doi.org/10.1016/j.jnca.2015.05.006
1084-8045/© 2015 Elsevier Ltd. All rights reserved.

energy resources (as DG, EV), demand response (DR) large-scale Renewable Energy Sources (RES), and ESS units (Weitemeyer et al., 2015). The ESSs have started to be used for multiple applications, such as wind and solar power smoothing, peak-shaving, frequency regulation, EV charging stations and others applications (Luo et al., 2015). In the short term, the ESS needs to fill the gap between the ramping down time of wind and solar and the ramping up time of these back-up plants. In addition, the main energy storage functionalities such as energy time-shift, quick energy injection and quick energy extraction are expected to make a large contribution to security of power supplies, power quality and minimization of direct costs and environmental costs (Zakeri and Syri 2015). The main challenge is to increase existing storage capacities and increase efficiencies and security.

The ESS can be integrated at different levels of the electricity system:

- Generation level: arbitrage, balancing and reserve power, etc.
- Transmission level: frequency control, investment deferral, etc.
- Distribution level: voltage control, capacity support, etc.
- User level: peak shaving, time of use cost management, etc.

The ESSs can inject/absorb the reactive power also and that can be the main control approach to mitigate voltage rise issue in distribution networks (Rouco and Sigrist, 2013). This feature can be managed by inverter's ESS using the available capacity at a specific moment in accordance with the demand of the electrical grid. This control is added to the regulation resources on-load tap changers. The experimental ESSs were based on electrochemical batteries on the grid lately. The BESSs offer a very dynamic system (Ma and Yang, Lu). It is adapted for power and energy applications. Actually, the BESS are used to develop the Micro-Grids and the future smart grid.

In the present paper the results of experimental activities performed on the prototype of BESS in order to test the reactive power compensation into the integration in a Micro-Grid available at the ENEA labs (Italian National Agency for New Technologies, Energy and Sustainable Economic Development) are reported. The reactive power control is part of CEI 0-16 and CEI 0-21, Italian standards defining the rules of connection of active and passive users to the grid (Delfanti et al., 2015). The aim of the monitoring activity was to define the best BESS's control in a Micro-Grid to provide ancillary services to the main grid, in particular, a reactive power service provided by the MV/LV transformer (Cavey et al., 2013). The later permits to use the BESS not only for energy and active power service but also to help the grid to stay stable and to increase the power quality in the presence of renewable generations. The experimental activities performed also deal with a special load that is an EV fast charging station included in the Micro-Grid: the survey has been extended to the control of the reactive and active power required by an EV fast charging station, giving the priority to the reactive power. The whole monitoring activities have been possible, thanks to the implementation of a customized communication and control system able to integrate the ESS with a smart metering system present into the Micro-Grid. The original point of this research is the analysis by using open protocols to manage a new service provided by the BESS. Further, a smart metering model has been developed and validated by experimental data to check the load of future systems.

2. Smart Grid and Micro-Grid: BESS integration

2.1. European case studies

Based on the content of the M/490 EU Mandate the CEN, CENELEC, and ETSI have been requested to develop a framework to enable European Standardization Organizations to perform continuous standard enhancement and development in the field of Smart Grids (Knapp and Samani, 2013). The EU wants to provide greater coherency of actions, as well as technological cooperation and a wider market. Energy storage is closely related to policy on renewable electricity. Here, member states have differing interests and possibilities and are at different stages of development (from near zero to over 50% of electricity generation). Support for storage within the EU internal electricity market and regulatory adjustments to enable storage facilitate the progress towards a single internal electricity market in Europe. Energy storage should be integrated into, and should be supported by, all relevant existing and future EU energy and climate measures and legislation, including strategies on energy infrastructure, the Connecting Europe Facility, RES promotion, Smart Cities and Communities, completion of the Internal Market, Energy Efficiency Directive, Horizon 2020, 2050 Roadmap, as well as the forthcoming discussion on a 2030 Strategy.

Different projects in EU have been founded to optimize and manage a wide range of different services that the storage can provide. These services need ICT infrastructure and a smart metering system. Some of these projects are provided here:

1) *Orkney Storage Park Project: In 2013 Mitsubishi Heavy Industries, Ltd. with Scottish Hydro Electric Power Distribution (SHEPD) created a demonstration project using the UK's Orkney Islands distribution grid* (Foote et al., 2013)*. The system capacity is 800 kW h nominal and the BESS is based on lithium*
2) *Saft Enel Substation Energy Storage Project: Saft's substation is located in the Puglia region of Italy, an area with a high level of variable and intermittent power from renewable energy sources that can cause reverse power flows on the high/medium voltage transformers. The role of Saft's lithium batteries in the ESS is to reduce the variability of power flow as well as allowing for more controllable energy exchange between the substation and the Italian national grid* (Bianco et al., 2015).
3) *Smarter Network Storage project: It is the largest such facility in Europe, a 6-MW/10-MW h lithium-ion battery storage project in U.K. The fully automated system is intended to provide balancing support for the grid and test how battery storage can make the network more efficient, as well as to improve the economics of battery storage systems and support the UK Carbon Plan* (Lidula and Rajapakse, 2011).

2.2. USA and rest of the world projects

Some smart grid projects are developing in USA and in the rest of the world. They provide an integration with the BESS. Some of these projects are reported here:

1) *The frequency regulation services and a firm wind project: AES is installing a 32 MW/8 MW h BESS based on lithium ion battery technology at the Laurel Mountain facility in West Virginia (USA).*
2) *CCET Technology Solutions for Wind Integration: Samsung SDI and Xtreme Power is installing a 1 MW to 1 MW h Lithium Ion based Battery Energy Storage System (BESS) system at the Reese Technology Center in Lubbock, Texas as part of a Smart Grid Demonstration Project (SGDP).*
3) *Fujian Electric Power Research Institute Mobile Energy Storage Station: the Fujian Electric Power Research Institute developed a mobile energy storage prototype project consisting of two sets of 125 KW/250 KW h battery systems and one of 125 KW/375 KW h hour battery system. The unit provides peak electricity for 10–15 commercial electricity consumers in the tea production industry* (Marmiroli et al., 2012).

Please cite this article as: Sbordone DA, et al. Reactive power control for an energy storage system: A real implementation in a Micro-Grid. Journal of Network and Computer Applications (2015), http://dx.doi.org/10.1016/j.jnca.2015.05.006

4) *The SDG&E Borrego Springs Microgrid Demonstration Project: The SDG&E microgrid project involves integration of five technologies, including distributed energy resources (DER) and VAR management, feeder automation system technologies (FAST), advanced energy storage, an outage/distribution management system, and price-driven load management. SDG&E installed a 1.5 MW h Li-ion battery energy storage system at the Borrego Springs Substation in June 2012.*
5) *Hokkaido Battery Storage Project: Kyodo News Service reported the authorization by Japan's Ministry of Economy, Trade and Industry for the installation of the world's largest storage battery, at a substation near several solar energy projects in Hokkaido Island, Japan, due to being online in March 2015.*

3. A real implementation of fast charging station with energy storage

A real implementation of a Micro-Grid has been designed, implemented and is now available at ENEA labs (Italian National Agency for New Technologies, Energy and Sustainable Economic Development). The global Micro-Grid structure is shown in Fig. 1. It is a further development of the system already presented by Sbordone et al. (2014). The Micro-Grid includes a prototype of BESS equipped with Li-batteries inverted-controlled and a special EV fast charging station (Falvo et al., 2013). A picture of the real system in ENEA labs, during the tests on Nissan EV charge, is reported in Fig. 2. All main devices inside the Micro-Grid and the used communication protocols as:

1. Battery Energy Storage System.
2. Smart metering devices.
3. EV charging station.
4. Modbus protocol.
5. Intranet data network.
6. CAN Protocol Communication.
7. Monitoring and control system;

are explained in the following paragraphs.

3.1. Battery Energy Storage System

The BESS consists of an active front end (AFE), with a 30 kV A nominal power, connected to the grid and to a DC low voltage bus-bar at 600 V through a DC link supplied by a 20 kW DC/DC buck booster and a Li-Polymer battery with 70 A h and 16 kW h total capacity. The Li-Ion batteries have a very high efficiency (95%) and energy density, and high number of life cycles (3.000–5.000). The power density of the Li-Ion battery is about 500 W/kg (discharge to 3C, 2500 W/kg) and the battery energy density is of 140 W h/kg. The BESS performance in terms of active power is limited by the characteristics of the batteries; they are able to give energy not more than 16 kW h in an hour and power not more than 20 kW for at least 30 min. The analyzed BESS is based on electrical scheme showed in Fig. 3.

The internal BESS control system communicates with external devices or control system through a CAN (Control Area Network) port and through CAN protocol. In this way, the external control system can read the internal status and measurements. The internal measurement devices to BESS consist of a 12 bit converter A/D and of a current transducer to measure battery current and exchanged current with the grid. The type is a LEM 100 P, with a measuring range 0 ± 150 A. The secondary nominal current is of 50 mA and it provides an accuracy of 0.45%. Further, the BESS can receive the values of set points for the active and reactive power. The bit rate of this communication has been fixed to 250 kbit/s. The BESS sends the status information on the bus CAN also. The batteries are managed by a Battery Management System (BMS). The BMS acquires the signals of cells voltage and temperature and

Fig. 2. The BESS inverted-controlled and the charge station during a test on a Nissan EV.

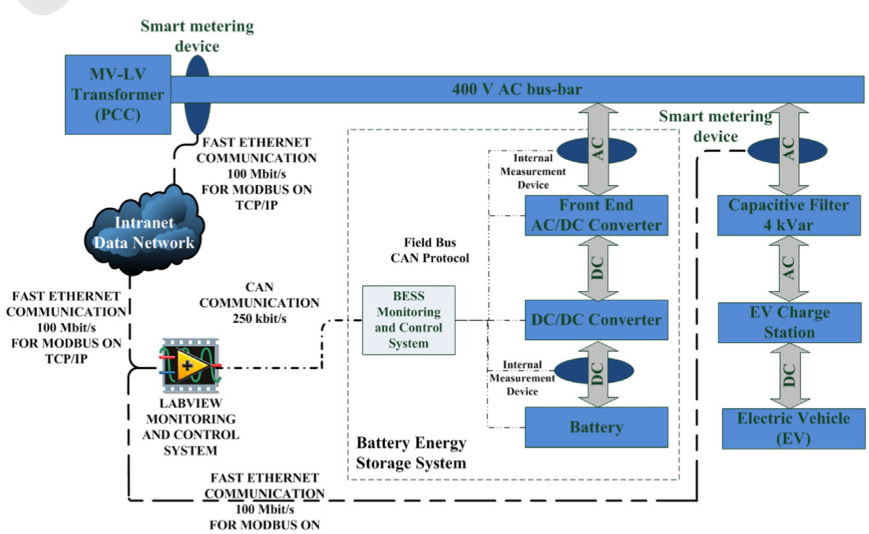

Fig. 1. Global system.

Please cite this article as: Sbordone DA, et al. Reactive power control for an energy storage system: A real implementation in a Micro-Grid. Journal of Network and Computer Applications (2015), http://dx.doi.org/10.1016/j.jnca.2015.05.006

so knows the batteries' state in every time instant. It also estimates the state of charge of the battery and gives information to the central system, through the CAN communication, on the battery state. Further, the main functions that BMS provides are charge/discharge current measurement; cell high voltage protection and alarm; cell low voltage protection and alarm; overcurrent protection and alarm; SOC calculation; cell equalization and balancing.

3.2. Smart metering devices

The smart metering devices cover a very important rule on the smart grid development. The European Commission issued a mandate M/441 for the standardization of smart metering functionalities and communication for usage in Europe for electricity, gas, heat and water applications that require the standardization process to ensure interoperability of technologies and applications within a harmonized European market. In order to address these challenges, the European Commission and EFTA addressed Mandate M/441 to CEN, CENELEC and ETSI (Lo Schiavo et al., 2013). The smart metering devices must provide the data in a precise way and with a very low time response. There are two smart metering devices interrogated by remote in this project. The first one is installed to measure the grid powers and it is an Electrex, X3M model. The latter uses the IEEE754 floating point representation on four bytes for the data saved in its internal registers. The second one is made by Control and the model is an EMM D3h 485. The data are integers on two bytes. An example of the internal data register is reported in Table 1. It is very important to notice the distance of the addresses in terms of bytes. Each request can receive maximum 8, 16 or 32 bytes based on the device. The Modbus on TCP/IP protocol can be used by both of them through a gateway. A performance analysis has been performed for the choice of communication protocol between two: serial and data network. It is reported in paragraph 5.

3.3. EV charging station

The EV charging station is a prototype, built by an industry on some specific given by an Italian and Spanish DSO, and ENEA that implements two modes of the EV fast charging in reference to the International Standard IEC 61851-1:

1) charging Mode 4 in DC, characterized by the use of off-board chargers, with an active power in output of 50 kW dc. The socket-outlet is an Yasaki Plug (ChadeMo protocol);
2) charging Mode 3 in AC, characterized by the use of on-board chargers, with an active power in output of 22 kW ac. The socket-outlet is a Type 2 socket-outlet (Mennekes protocol).

Typical charging times of the mode 4 are in a range from 20 to 30 min. In this case the charging time is limited by the allowable current of 125 A and voltage of 500 V on the CHAdeMO connector. Further details are reported in (Sbordone et al., 2014). This experimentation used a filter of 4 kVar to avoid high values of THD.

3.4. Network infrastructure

The network infrastructure is made by different protocols that permit the integration of different systems and devices. The Monitoring and control system uses the following open protocols:

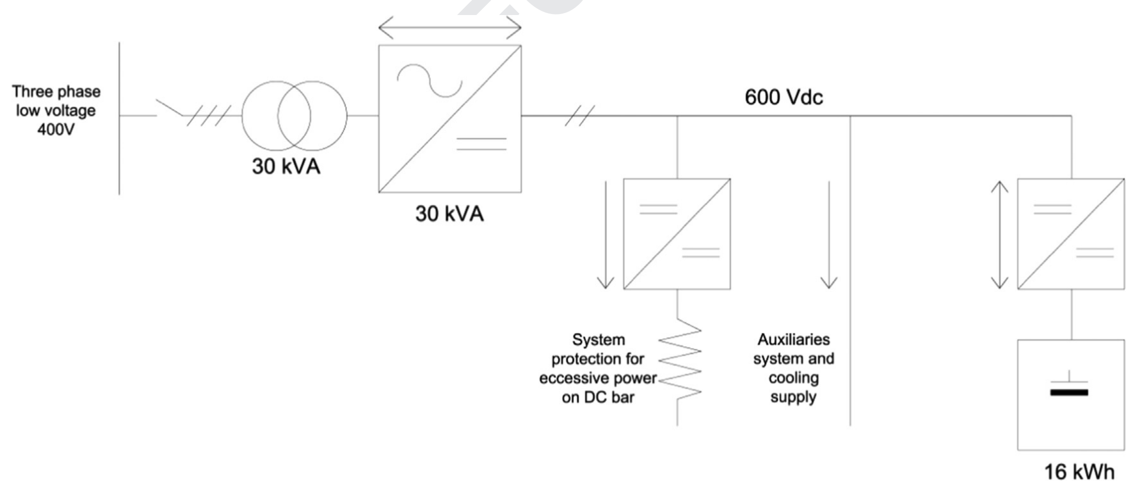

Fig. 3. Scheme of BESS.

Table 1
Internal data register of a smart metering device.

Addr.	Type	Description	Unit	Symbol	Config
214–215	Float IEEE754	Phase to Neutral Voltage, RMS Amplitude	V	U_{1N}	3P4W, 1P2W
216–217	Float IEEE754	Phase to Neutral Voltage, RMS Amplitude	V	U_{2N}	3P4W
218–219	Float IEEE754	Phase to Neutral Voltage, RMS Amplitude	V	U_{3N}	3P4W
220–221	Float IEEE754	Phase to Neutral Voltage, RMS Amplitude	V	U_{12}	3P4W, 3P3W
222–223	Float IEEE754	Phase to Neutral Voltage, RMS Amplitude	V	U_{23}	3P4W, 3P3W
224–225	Float IEEE754	Phase to Neutral Voltage, RMS Amplitude	V	U_{31}	3P4W, 3P3W
234–235	Float IEEE754	Phase Active Power (±)	W	P_1	3P4W, 1P2W
236–237	Float IEEE754	Phase Active Power (±)	W	P_2	3P4W
238–239	Float IEEE754	Phase Active Power (±)	W	P_3	3P4W
240–241	Float IEEE754	Phase Active Power (±)	var	Q_1	3P4W, 1P2W

Please cite this article as: Sbordone DA, et al. Reactive power control for an energy storage system: A real implementation in a Micro-Grid. Journal of Network and Computer Applications (2015), http://dx.doi.org/10.1016/j.jnca.2015.05.006

- Modbus protocol.
- TCP/IP and Ethernet protocols.
- CAN protocol.

The Modbus is a simple and robust serial communications protocol. It has become a de facto standard communication protocol, and is now a commonly available means of connecting industrial electronic devices (Hui et al., 2012). The main reasons for the use of Modbus in the industrial environment are:

- developed with industrial applications in mind,
- openly published and royalty-free,
- easy to deploy and maintain,
- moves raw bits or words without placing many restrictions on vendors.

Modbus enables communication among many (about 250) devices connected to the same network and it has been used to connect the supervisory monitoring and control system to the remote terminal unit (RTU). The Modbus requests have been performed by the monitoring and control system on the TCP/IP network through a gateway. The latter is a part of a very large intranet. However all devices and the monitoring and control system are on the same subnet with an IP address of C class. They are connected through Fast Ethernet (100 Mbit/s) connection to the Cisco catalyst switches with medium load. Further, the data are transmitted through only two switches and do not jump any routers. No quality of service is implemented on the switches for the Ethernet frames sent by the devices and by the monitoring and control system. Further, the monitoring and control system uses the CAN protocol that is a multi-master serial bus standard for connecting Electronic Control Units also known as nodes. Two or more nodes are required on the CAN network to communicate. Each node is able to send and receive messages, but not simultaneously. It is defined by ISO 11898-2/3 Medium Access Unit standards (Mubeen et al., 2014). A message consists primarily of the Id (identifier), which represents the priority of the message, and up to eight data bytes. The BESS uses CAN as a field protocol. The monitoring and control system has been interfaced to the BESS through a PEAK USB-CAN device. The bit rate of this

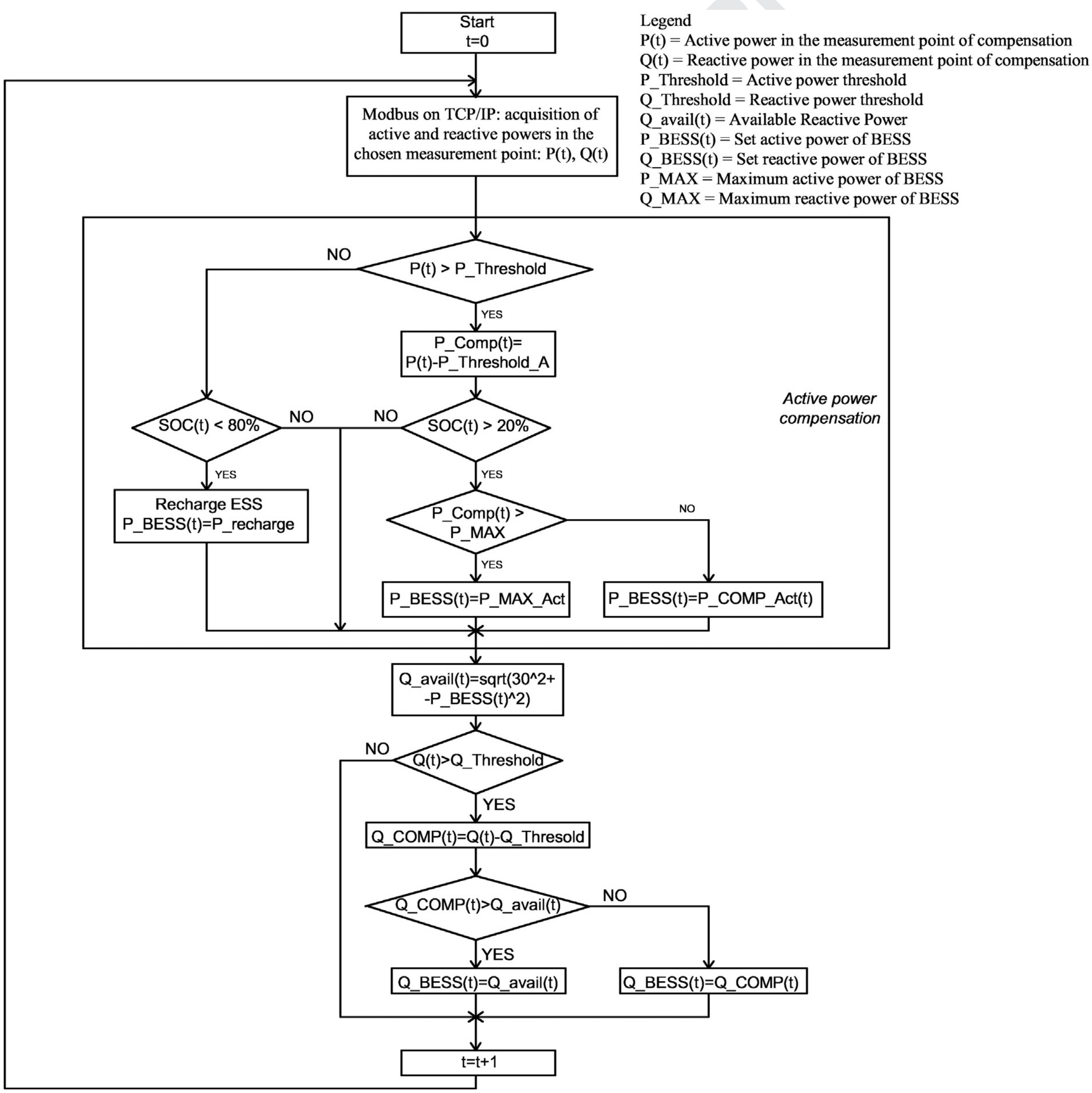

Fig. 4. First compensation logic: active power priority control.

Please cite this article as: Sbordone DA, et al. Reactive power control for an energy storage system: A real implementation in a Micro-Grid. Journal of Network and Computer Applications (2015), http://dx.doi.org/10.1016/j.jnca.2015.05.006

communication has been fixed to 250 kbit/s, and the set data can be provided every 10 ms on a determinate identification message providing it the values of active and reactive power in every time instant. Further, it is possible to read some messages sent by BESS to check the status of the system and read some measurements. Some of these CAN messages sent by the BESS are:

- Id 0x19F0CC59: every 100 ms the total battery voltage, the total battery current and the state of charge (SOC).
- Id 0x0200: every 10 ms the grid voltage and the current of single phases.
- Id 0x0201: every 10 ms active and reactive power, the frequency and the BUS DC voltage.
- Id 0x0180: every 50 ms the active and reactive power of the ESS.

3.5. Monitoring and control system

The monitoring and control system has been developed in Labview of National Instruments. Labview has been chosen as a simple way to interface different communication protocols in the same developing environment. The monitoring and control system is connected:

1) To the smart metering devices through fast Ethernet connected by the intranet data network;
2) To the BESS via CAN protocol with a bit rate fixed to 250 kbit/s.

The program has been developed on a PC based on windows. It can offer a near-real time control, but it cannot be considered a real time system because the operative system performs other task at the same time. The measurements acquired through that system are:

- active power that the BESS exchanges with the grid;
- reactive power that the BESS exchanges with the grid;
- active power provided by the grid;

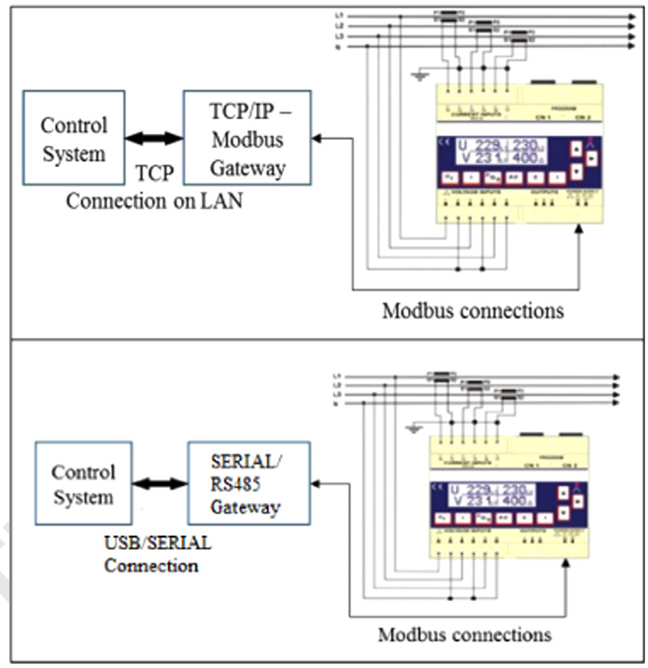

Fig. 6. Tested configurations for smart metering performances.

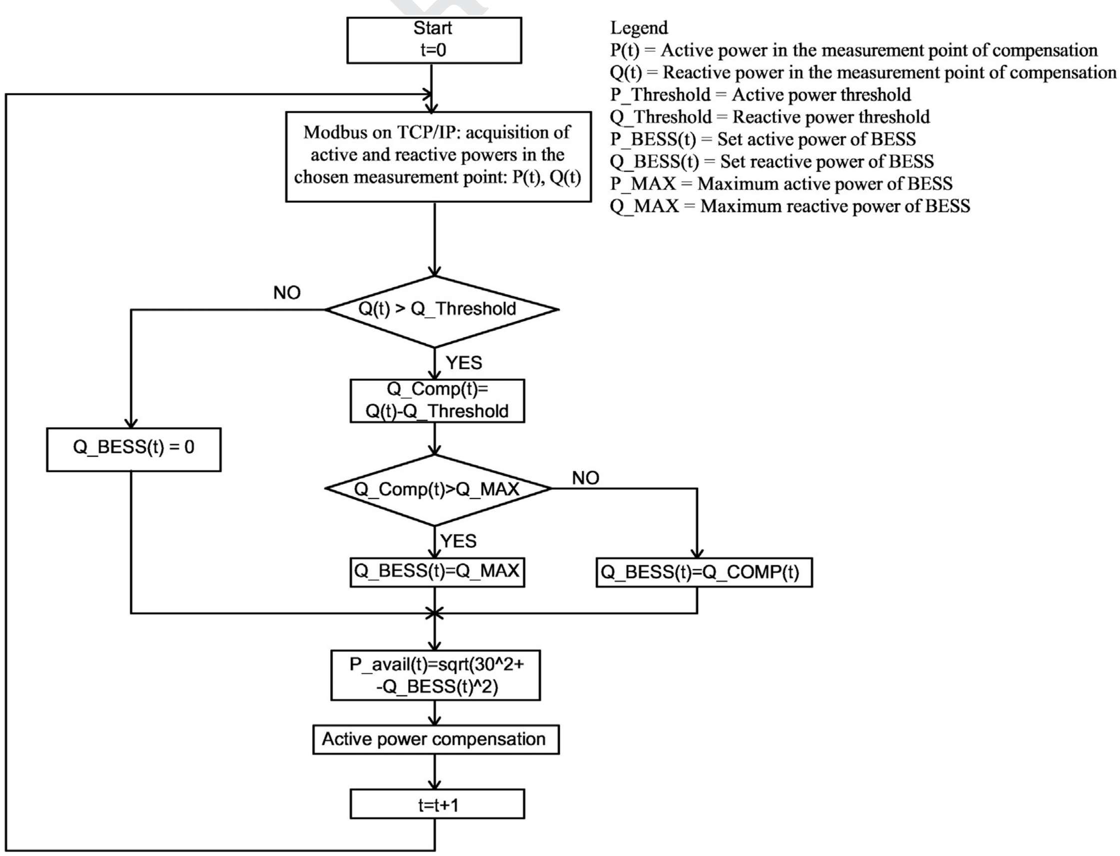

Fig. 5. First compesation: reactive power.

Please cite this article as: Sbordone DA, et al. Reactive power control for an energy storage system: A real implementation in a Micro-Grid. Journal of Network and Computer Applications (2015), http://dx.doi.org/10.1016/j.jnca.2015.05.006

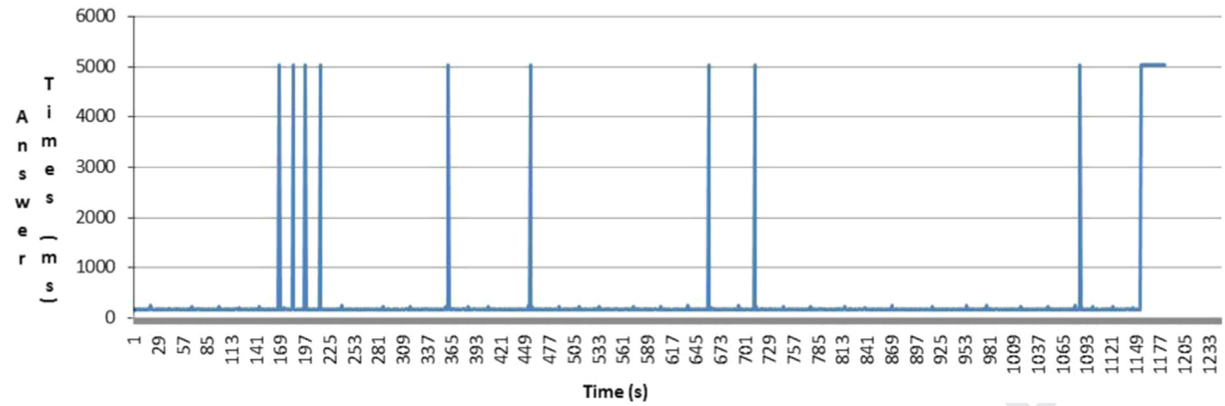

Fig. 7. Answer time for serial with 25 ms of delay in the loop.

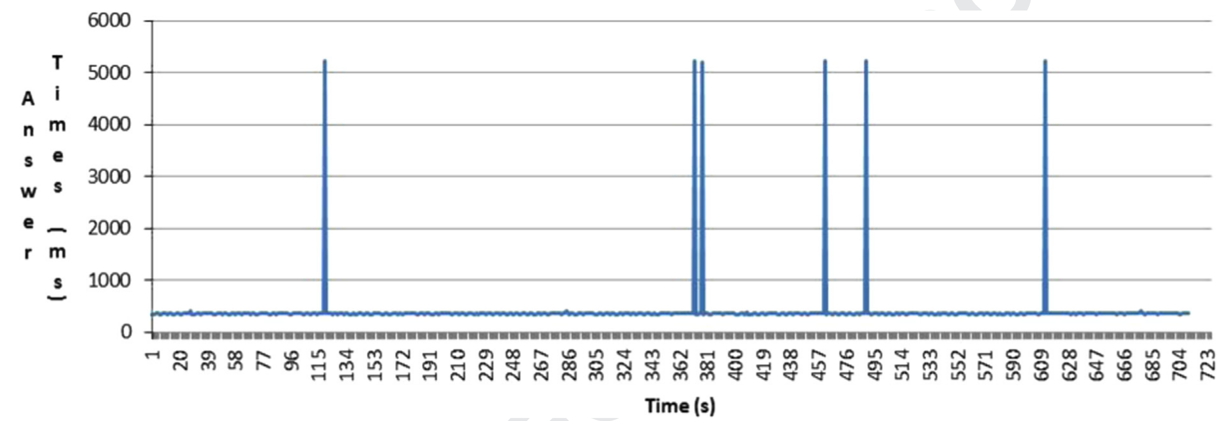

Fig. 8. Answer time for serial with 200 ms of delay in the loop.

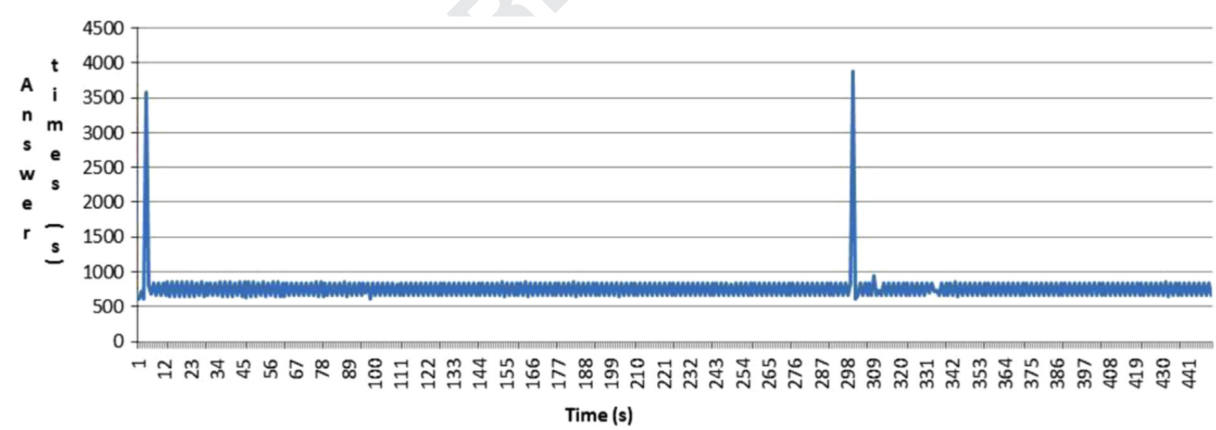

Fig. 9. Device 1: answer time for network with 200 ms of delay in the loop.

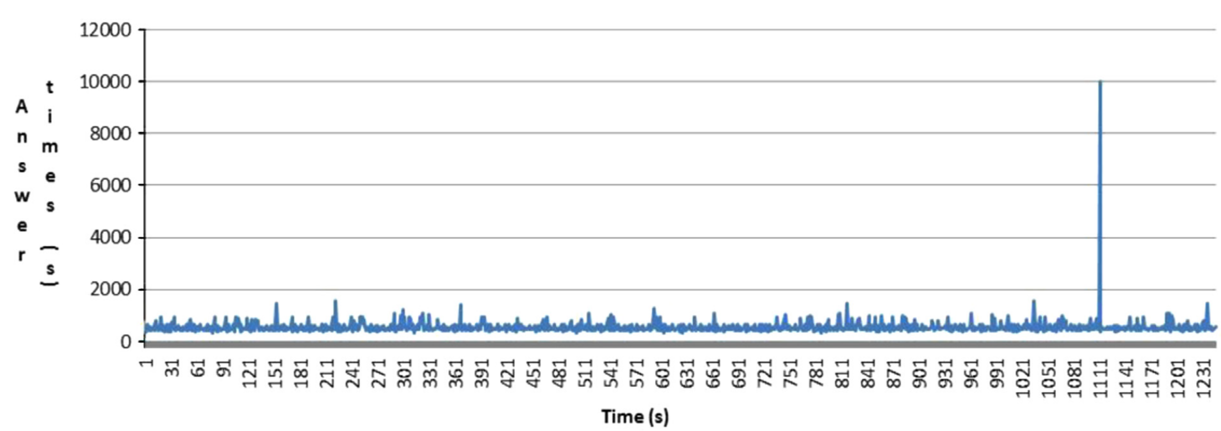

Fig. 10. Device 2: answer time for network with 200 ms of delay in the loop.

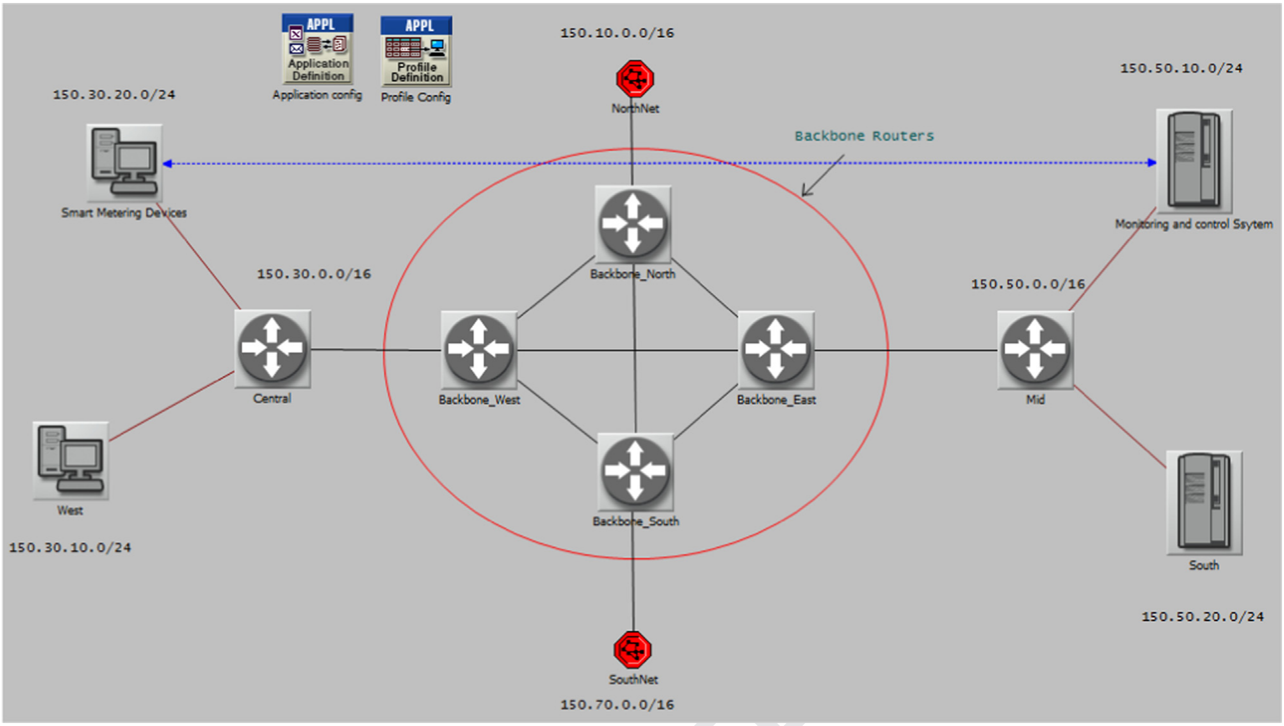

Fig. 11. Network infrastructure model.

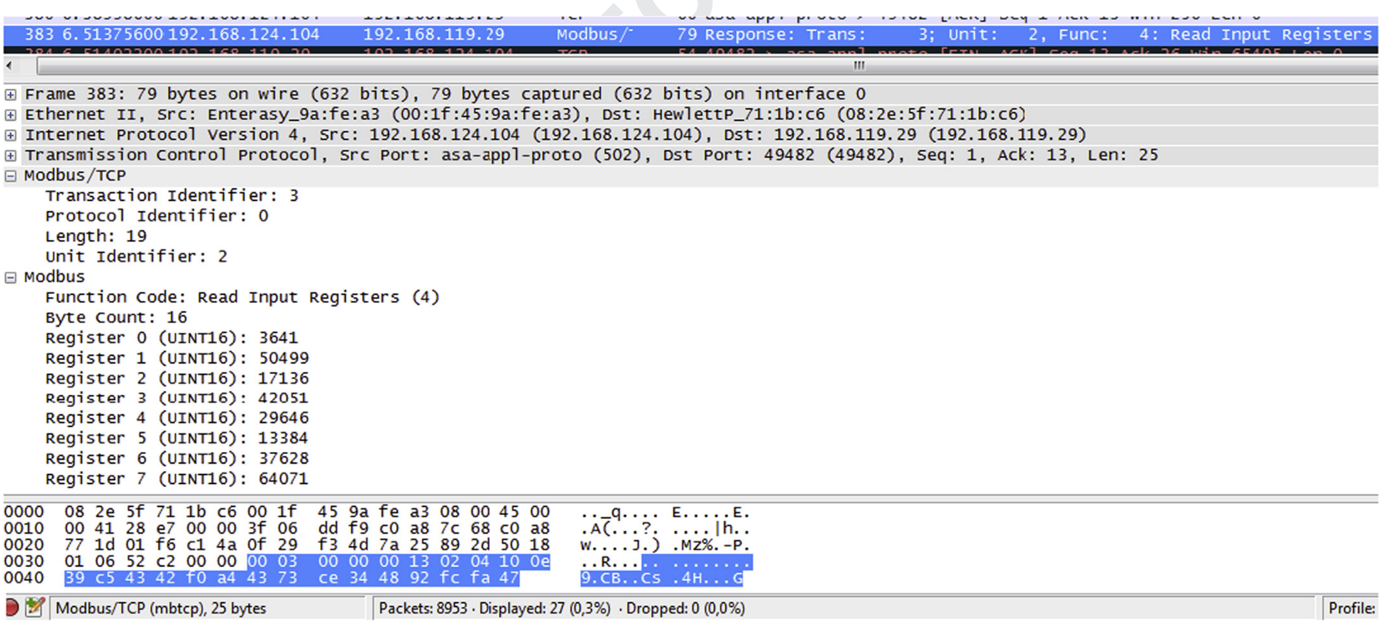

Q7 **Fig. 12.** Modbus information exchange. (For interpretation of the references to color in this figure, the reader is referred to the web version of this article.)

- reactive power provided by the grid;
- voltage of bus-bar;
- active power that the EV charge station absorb by the grid;
- reactive power that the EV charge station absorb by the grid;
- voltage on the load connection;
- active power that the battery provides or absorbs by the DC/DC converter;
- the status of the battery through the battery management system (BMS) of the BESS.

4. The control logics

The experimented control logics have developed two algorithms.

4.1. Active power compensation priority control

The first logic gives priority to the active power compensation. A flow chart summarizing this type of control is shown in Fig. 3.

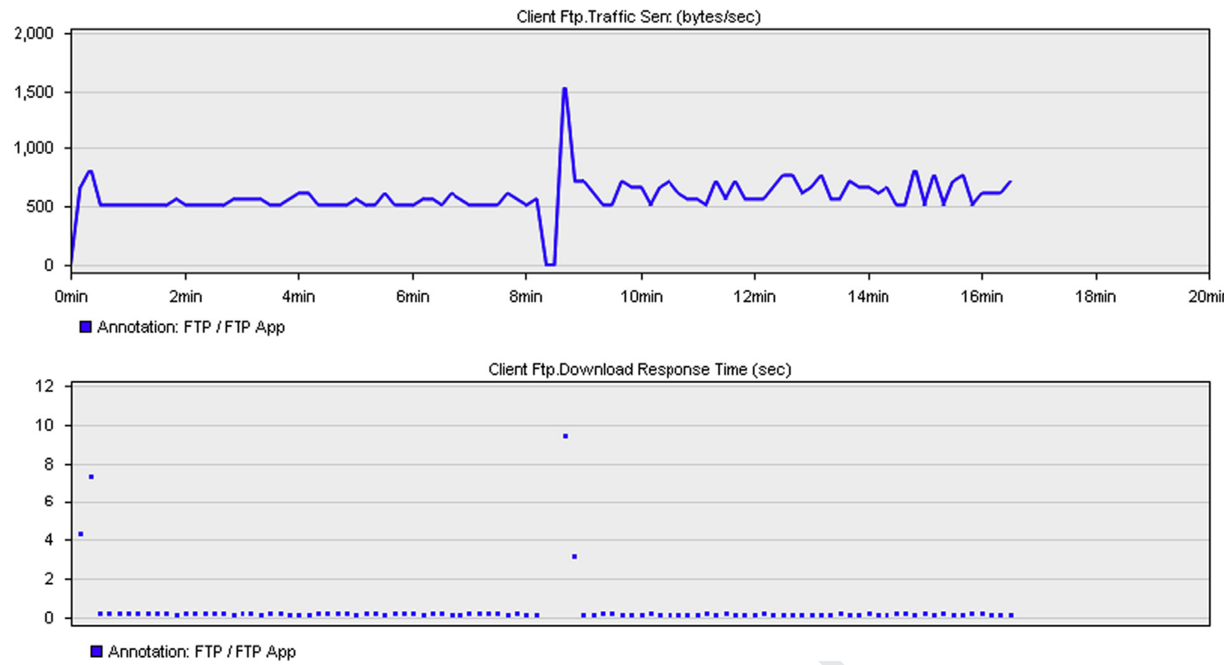

Fig. 13. Single smart metering device and single request.

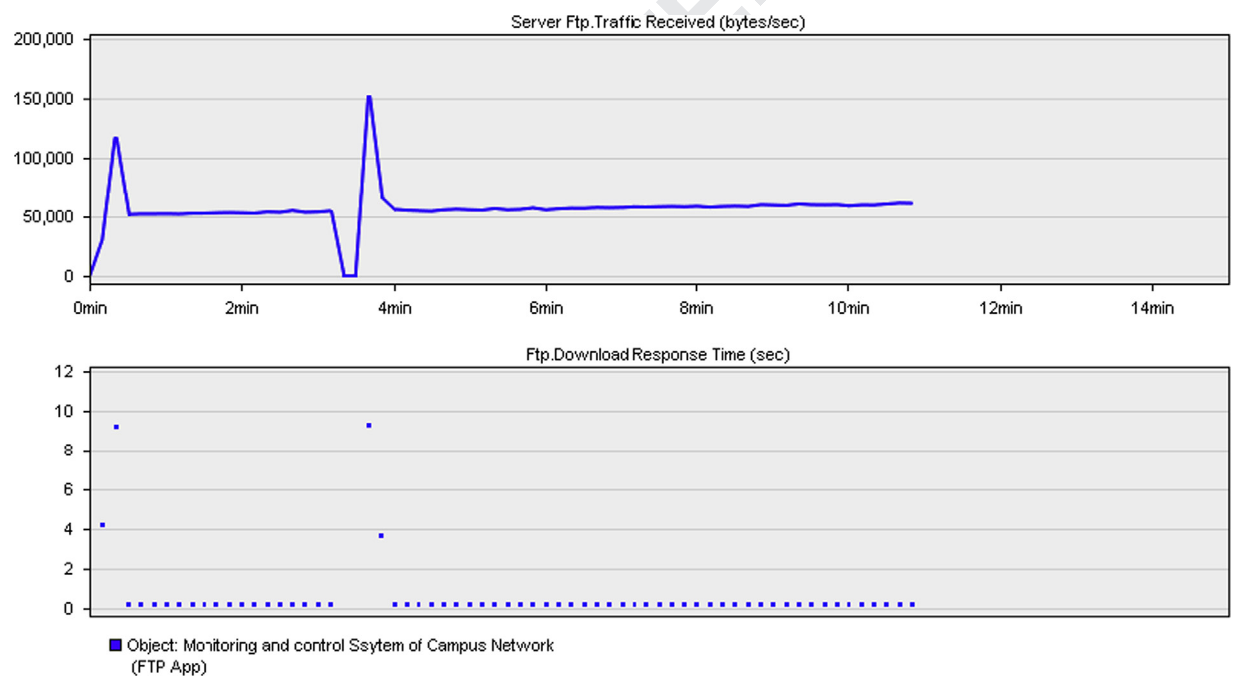

Fig. 14. One hundred of smart meter device and a single aggregator.

The active power control performs a peak shaving logic that has been already tested and explained by the authors in Sbordone et al. (2014). The monitoring and control system read the active and the reactive power in the measurement point. If the power absorbed in the measurement point is greater than a settled threshold and the BESS SOC is in the range 20–80%, the BESS provides the power given by the difference between the total power provided by the grid and the threshold. The result is limited to maximum active power of BESS. Further, it also manages the reactive power. If the inverter's BESS does not provide all the available apparent power, the control system calculates the available reactive power ($Q_{av}(t)$); it can provide or absorb based on the measures through the equation:

$$Q_{av}(t) = \sqrt{30^2 - P_{BESS}^2(t)} \tag{1}$$

where the 30 kVA power value is the maximum apparent power of the BESS in Eq. (1). If the reactive power absorbed in the measurement point is greater than a settled reactive power threshold, the BESS provides the reactive power given by the difference between the reactive power provided by the grid and the threshold. The result is limited to the maximum reactive power available in that moment from the BESS. The reactive power can be negative and so the algorithm applies the same

Please cite this article as: Sbordone DA, et al. Reactive power control for an energy storage system: A real implementation in a Micro-Grid. Journal of Network and Computer Applications (2015), http://dx.doi.org/10.1016/j.jnca.2015.05.006

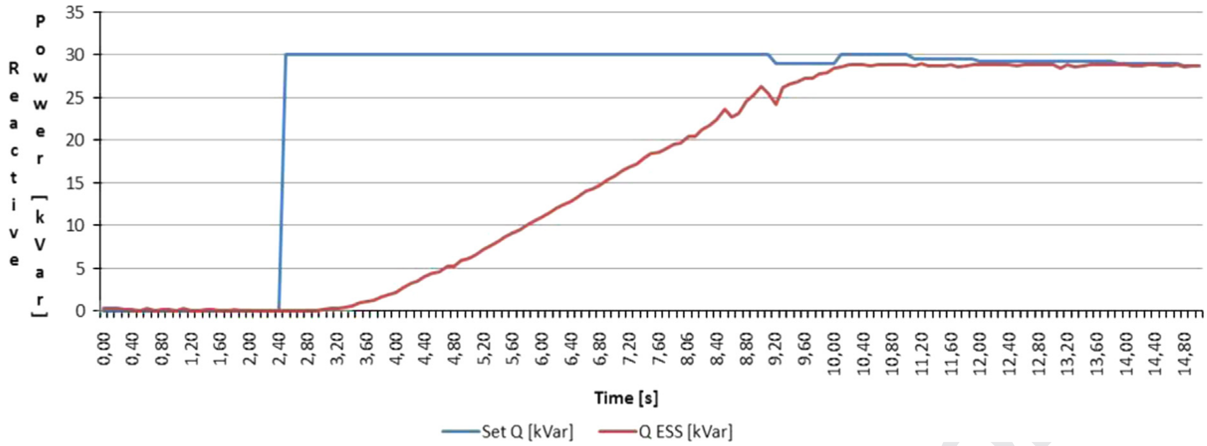

Fig. 15. BESS answer time for the reactive power compensation.

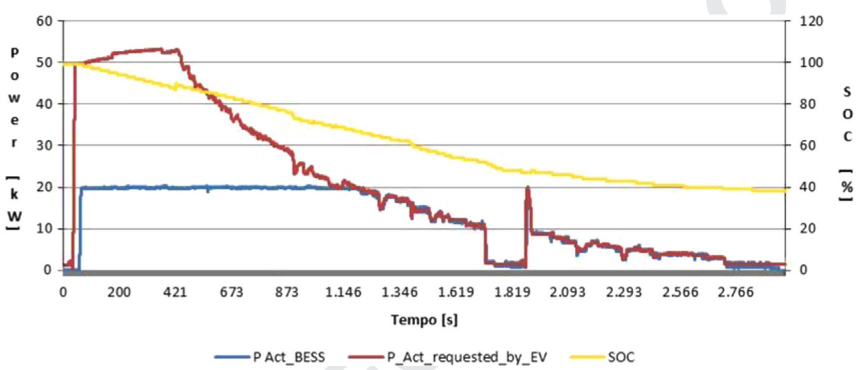

Fig. 16. Active power compensation.

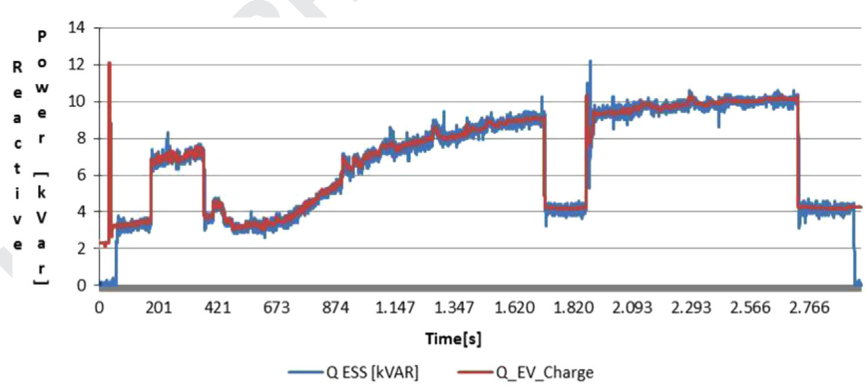

Fig. 17. Reactive power compensation.

logic for a negative threshold. To simplify, it has been reported only in the case where the reactive power is positive.

4.2. Reactive power compensation priority control

The second algorithm gives the priority to the reactive power. A flow chart summarizing this type of control is shown in Fig. 5. The monitoring and control system reads the active and the reactive power in the measurement point. If the absorbed reactive power is greater than a settled threshold in the measurement point, the BESS provides the reactive power given by the difference between the reactive power provided by the grid and the threshold. The result is limited to maximum reactive power of inverter's BESS. Successively, the control system calculates the available active power that is available ($P_{av}(t)$) through Eq. (2). If it is possible, the control system performs the peak shaving (active power compensation) with this power.

$$P_{avl}(t) = \sqrt{30^2 - Q_{BESS}^2(t)} \quad (2)$$

5. Smart metering performances

The Modbus protocol has been chosen for the interoperability scope in this project as seen before. Further, a time answer analysis of different interfaces and of the different devices has been performed. This analysis is needed for the choice of time loop in the monitoring and control program. The Modbus protocol has

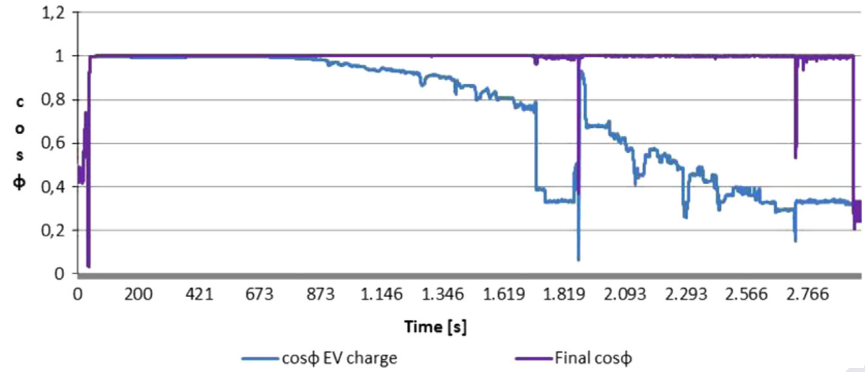

Fig. 18. Power factor with and without compensation. (For interpretation of the references to color in this figure, the reader is referred to the web version of this article.)

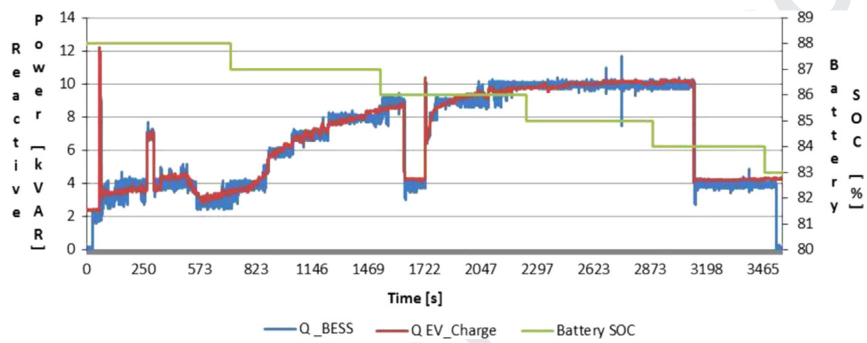

Fig. 19. Reactive power compensation.

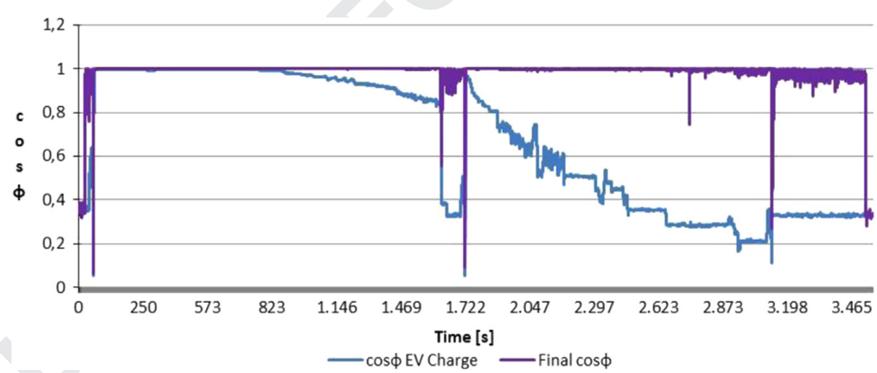

Fig. 20. Power factor.

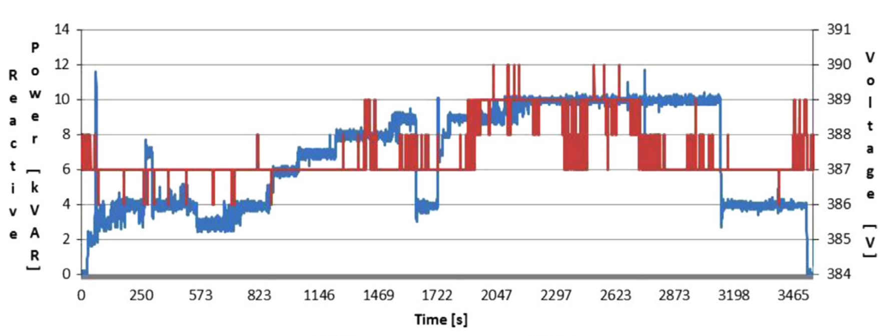

Fig. 21. Effects on voltage.

been tested on the serial port and on the data network connection. The tested connections are shown in Fig. 6.

A Labview program has been developed only for this part. The test program takes in account the starting timestamp just before that the Modbus request is ready. Successively it sends the data to the smart metering device and it waits for the answer. The final timestamp is saved when the answer is received by the control program. So the answer time is given by the difference between the final timestamp

Please cite this article as: Sbordone DA, et al. Reactive power control for an energy storage system: A real implementation in a Micro-Grid. Journal of Network and Computer Applications (2015), http://dx.doi.org/10.1016/j.jnca.2015.05.006

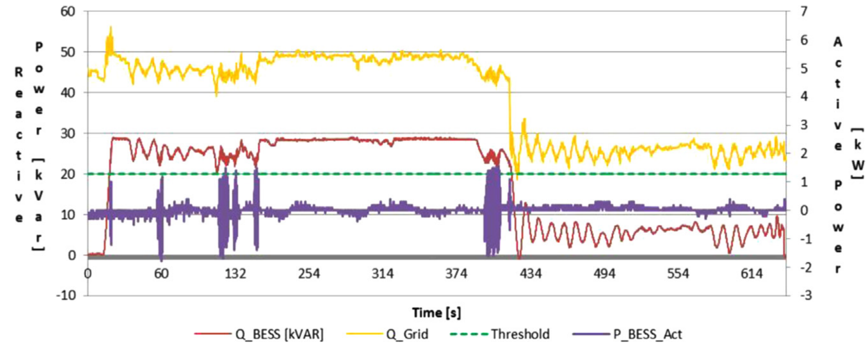

Fig. 22. First reactive compensation.

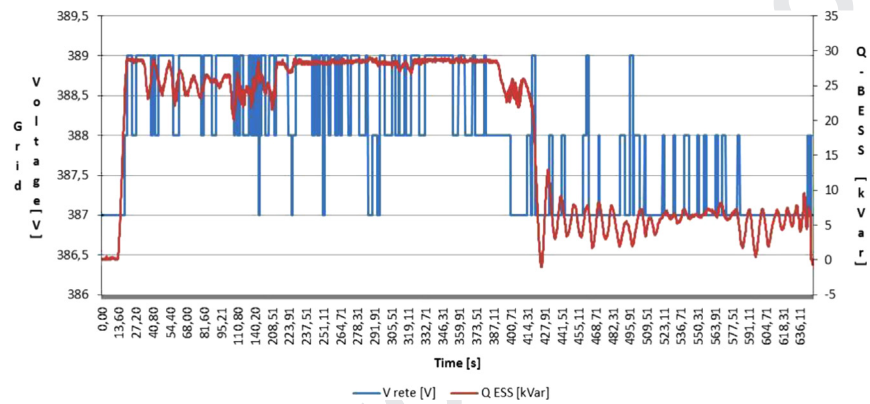

Fig. 23. Effects on grid voltage.

and the starting timestamp. Further a variable delay has been inserted between a request and another in the loop.

The first analysis shows the answer times for Modbus requests on serial port for a smart metering device. Each request is delayed for 25 ms. Indeed many timeouts take place if a delay in the loop is not inserted. Fig. 7 shows that the device sometimes goes in the timeout. The answer times arrive to 5 s in that case. The lost requested measurements are 1% of the total with an average answer time of 300 ms.

Another analysis has increased the loop delay of 200 ms. The result is shown in Fig. 8.

Some requests go in time out in this case also. The percentage of lost requested measurements is 0.84% with an average answer time of 400 ms. The second analysis shows the answer times for Modbus request on TCP/IP for the same device. Of course the latter is preferred because it offers longer connection cable and a data rate higher than serial port. As shown in Fig. 9 the percentage of lost measurements is 0.40% with an average answer time of 760 ms.

The same analysis has been performed for the other devices present in ENEA as shown in Fig. 10. In this case the percentage of lost measurement is 0.07% with an average answer time of 550 ms.

6. Smart metering model

A model has been developed by referring to the experimental data. The network and the service on a more complex infrastructure has been replicated to understand the implication in terms of baud rate and delay. The network infrastructure model is shown in Fig. 11. The monitoring and control system is shown on right side while the smart metering device is shown on the left side.

Openet has been used to perform this analysis and other research on this field (Panchadcharam et al., 2012). The software does not provide the Modbus on TCP/IP protocol tools but the FTP protocol features have been adapted to simulate it. Fig. 12 shows all messages for a request through Modbus on TCP/IP protocol acquired by Wireshark tool. The all encapsulated bites sent by Modbus request are 1488. The bites received by the server are 1588 for each request.

The FTP protocol has been chosen because it is a protocol based on connection and it has been configured to transmit the same byte numbers checked experimentally with Modbus requests. The probability to the losses has also been set and a simple case is shown in Fig. 13. Indeed, it is shown that after about 8 min the smart metering device goes in timeout and no data is transmitted.

The average traffic is about 500 bytes/s for the single device. A second test has been performed to evaluate the baud rate and the delay for an aggregator that interrogates 100 smart metering devices. The results are shown in Fig. 14.

As shown, a single aggregator can support many smart meters without problems using a low bandwidth. The latter has been 50 kbytes/s with 100 smart meters. Of course the delay can change based on the network load and a different quality of service can be applied to minimize it. This last depends from the control system. In developed control system the loop time has been set to 1 s based on the smart metering performances. Further the devices are interrogated by the control system two times in the same loop to acquire different values too much distant in terms of Modbus registers.

7. Experimental tests on the real system

The control system loop time has been set to 1-s based on the smart metering performances. Further the devices are interrogated by the control system two times in the same loop to acquire different values too much distant in terms of bytes. That choice avoids timeouts for smart metering devices and it avoids high packet loss rate and are degraded throughput due to the ineffectiveness for TCP congestion (Khalifa et al., 2014). However, the control system manages the timeout using the previous acquired value.

The first experimental activity has provided the answer time of the system under maximum perturbation. This shows that the system adapts itself and how much time is required. The other experimentations have tested the two algorithms on two different measurement points shown in Fig. 1: one on the EV charge load and the other on the grid.

7.1. BESS answer time in reactive power compensation

This experimentation shows the dynamic behavior of the system under maximum perturbation. The experimental data are provided in Fig. 11. Starting from 0 to provide the maximum reactive power, the system takes about 10 s to reach the maximum value and stabilize itself.

7.2. Active power compensation priority control for a special load

The experimental test deals with the use of the system for the charging of an EV: a Nissan Leaf car. It is an electric car manufactured by Nissan and it has an autonomy of 200 km. This EV is equipped with a Li-Ion battery pack with a nominal energy of 24 kW h and a nominal peak power of 90 kW. The charging time according to fast charge is about 30 min with a recharge from 0% to 80%. The algorithm in Fig. 4 has been used in this test. The experimented control logic system has tested implementing a peak shaving algorithm. Fig. 12 shows the active power compensation performed by the BESS during the charge of the EV through the charge station. The real data acquisition for the first test shows that

- the red curve gives the profile of the power required by EV for the battery charging (left axis values);
- the blue curve gives the profile of the power given by the BESS (left axis values);
- the yellow curve gives the SOC of the BESS (right axis values).

The maximum active power provided by the BESS is 20 kW. So, a quantity of reactive power is available to be used. Indeed the control system can use that reactive power and the result is shown in Fig. 13. Fig. 13 shows as the reactive power requested by the EV fast charge can be provided by the BESS. In this way the power factor is close to 1. The power factor with and without compensation is shown in Fig. 14.

Q3 7.3. Reactive power compensation priority control for a special

In this experimentation the priority to the reactive power has been given. As seen before, the BESS can compensate the active and reactive power on the EV fast charge. A high active power threshold has been chosen in this experimentation to avoid active power compensation. So the energy consumption to cover the reactive power compensation service has been analyzed. Fig. 15 shows the reactive power absorbed by the EV charge and the reactive power provided by the BESS. Further Q4 this figure shows the BESS's SOC. It starts from 88% and it arrives to 83%. That means an energy consumption by the BESS's batteries of 800 W h.

Fig. 16 shows the power factors with and without the reactive power compensation. Fig. 17 shows the effects on the voltage grid to the reactive power compensation.

7.4. Active power compensation priority control for the main grid

The last experimentation gets the measures to compensate from the grid's point of view, as shown in Fig. 1. The control system applies the algorithm shown in Fig. 5 to compensate the reactive power first. The results are shown in Fig. 18 where

- the yellow curve gives the profile of the reactive power supplied by the grid (left axis values);
- the red curve gives the profile of the reactive power given by the BESS (left axis values);
- the blue curve gives the profile of the active power given by the BESS (right axis values);
- the green curve gives the reactive power threshold (left axis values).

The BESS provides almost 30 kVAR in the first 400 s. So the BESS was not available for active power to perform any active power compensation. Successively, the reactive power requested by the loads decreases, and the requested active power also decreases. Indeed it does not over the active power threshold and so the BESS does not compensate any active power. In Fig. 19 the grid voltage and the reactive power provided by the BESS are reported. Of course the BESS is only of 30 kV A and the MV/LV transformer is of 1000 VA. These effects are not always visible because it depends from the total load on the grid in that moment (Figs. 20–23). Q5

8. Conclusions

A real Micro-Grid with a Lithium Battery Energy Storage System (BESS) has been deeply described. The Micro-Grid has been implemented and available at ENEA labs (Italian National Agency for New Technologies, Energy and Sustainable Economic Development). A wide experimental activity has been performed on the system in order to test the reactive power compensation of a BESS. That has requested the full integration of the system between EV charging station, BESS and smart metering system. The latter has been modeled and its performances have been analyzed in terms of answer times and baud rate. The analysis has allowed sizing the loop time in the control system to obtain the synchronization of the different entities of the Micro-Grid. The integration of smart metering system and the control system has been possible, thanks the use of open ICT protocols and a customized LabView program also. The Modbus on TCP/IP connection has been chosen because the smart meter devices can be far from the monitoring and control system. The TCP/IP protocol guarantees the communication for any distance with limited delay. The results of the experimental tests have shown that the developed system is able and shows good performance into the implementation of reactive power compensation for the EV charging station. Indeed the power factor for that load can become unitary. The BESS does not have the right size to affect the grid voltage in the grid reactive power compensation. Considering all experimental activities, the system can be considered the nucleus of a more complex power system, including distributed ESS, to test the performance of a so-made system is the second step for implementing a methodology for the siting and sizing of a distributed BESS on a AC distribution network including ancillary services.

References

Arboleya P, Gonzalez-Moran C, Coto M, Falvo MC, Martirano L, Sbordone D, et al. Efficient energy management in smart micro-grids: ZERO grid impact buildings. Smart Grid IEEE Trans 2015;6(2):1055–63.

Bianco G, Noce C, Sapienza G. Enel Distribuzione projects for renewable energy sources integration in distribution grid. Smart Grids Worlds Actual Implement 2015;120(0):118–27.

Cavey, MV, Helsen, L, Tant, J, Geth, F, Driesen, J. Real-time control for services provided by battery energy storage systems in a residential low voltage grid with a large amount of PV. In: Proceedings of the 22nd international conference and exhibition on electricity distribution CIRED 2013; 2013. p. 1–4.

Delfanti M, Falabretti D, Fiori M, Merlo M. Smart Grid on field application in the Italian framework: the A.S.S.E.M. project. Smart Grids Worlds Actual Implement 2015;120(0):56–69.

Falvo, MC, Martirano, L, Sbordone, D, Bocci E. Technologies for smart grids: a brief review. In: Proceedings of the 12th international conference on environment and electrical engineering, EEEIC 2013. May; 2013. p. 369–75.

Falvo, MC, Martirano, L, Sbordone, D, Bertini, I, Di Pietra, B, Vellucci, F. A flexible Customer Power Device for energy management in a real Smart Micro-Grid. In: Proceedings of the 39th annual conference of the IEEE industrial electronics society IECON-2013. November;. 2013. p. 7586–91.

Foote, C, Johnston, R, Watson, F, Currie, R, MacLeman, D, Urquhart, A. Second generation active network management on Orkney. In: Proceedings of the 22nd international conference and exhibition on electricity distribution CIRED 2013. 2013. p. 1–4.

Huang Yingsong, Mao Shiwen, Nelms RM. Adaptive electricity scheduling in microgrids. Smart Grid IEEE Trans 2014;5(1):270–81.

Hui, L, Hao, Z, Daogang, P. Design and application of communication gateway of EPA and MODBUS on electric power system. In: Proceedings of the 2012 international conference on future electrical power and energy system. vol. 17, Part A, no. 0; 2012. p. 286–92.

Jackson J. Chapter 28 - smart grids: an optimised electric power system. editor. In: Letcher TM, editor. Future energy. Second edition Boston: Elsevier; 2014. p. 633–51 In:.

Khalifa T, Abdrabou A, Shaban KB, Alsabaan M, Naik K. Transport layer performance analysis and optimization for smart metering infrastructure. J Netw Comput Appl 2014;46(0):83–93.

Knapp ED, Samani R. “Chapter 5 - security models for SCADA, ICS, and smart grid,”. In: Knapp ED, Samani R, editors. Applied cyber security and the smart grid. editors. Boston: Syngress; 2013. p. 101–23.

Lidula NWA, Rajapakse AD. Microgrids research: a review of experimental microgrids and test systems. Renew Sustain Energy Rev 2011;15(1):186–202.

Lo Schiavo L, Delfanti M, Fumagalli E, Olivieri V. Changing the regulation for regulating the change: innovation-driven regulatory developments for smart grids, smart metering and e-mobility in Italy. Energy Policy 2013;57(0):506–17.

López MA, de la Torre S, Martín S, Aguado JA. Demand-side management in smart grid operation considering electric vehicles load shifting and vehicle-to-grid support. Int J Electr Power Energy Syst 2015;64(0):689–98.

Luo X, Wang J, Dooner M, Clarke J. Overview of current development in electrical energy storage technologies and the application potential in power system operation. Appl Energy 2015;137(0):511–36.

Ma, T, Yang, H, Lu, L. Development of hybrid battery–supercapacitor energy storage for remote area renewable energy systems. Appl energy, no. 0.

Marmiroli, M, Koshio, M, Tsukamoto, Y. Japanese test facilities for smart grid. In: proceedings of the IEEE international conference on smart grid engineering SGE 2012; 2012. p. 1–7.

Mubeen S, Mäki-Turja J, Sjödin M. MPS-CAN analyzer: Integrated implementation of response-time analyses for Controller Area Network. J Syst Archit 2014;60(10):828–41.

Panchadcharam, S, Taylor, GA, Ni, Q, Pisica, I., Fateri, S. Performance evaluation of smart metering infrastructure using simulation tool. In: Proceedings of the 47th international universities′ power engineering conference UPEC 2012. September; 2012. p. 1–6.

Pillai, JR, Thogersen, Shaojun Huang P, Moller, J, Bak-Jensen, B. Electric vehicles in low voltage residential grid: a Danish case study. In: Proceedings of the 3rd IEEE PES international conference and exhibition on innovative smartgrid technologies ISGT Europe; 2012. p. 1–7.

Rouco, L Sigrist, L. Active and reactive power control of battery energy storage systems in weak grids. In: Proceedings of the 2013 IREP symposium on bulk power system dynamics control - IX optimization security and control emerging power grid IREP; 2013. p. 1–7.

Sbordone D, Bertini I, Di Pietra B, Falvo MC, Genovese A, Martirano L. EV fast charging stations and energy storage technologies: a real implementation in the smart micro-grid paradigm. Electr Power Syst Res 2014. Q6

Skopik, F., Friedberg, I., Fiedler, R. Dealing with advanced persistent threats in smart grid ICT networks. In: Proceedings of the 2014 IEEE PES innovative smart grid technologies conference ISGT; 2014. p. 1–5.

Liang Tao, C. Schwaegerl, S. Narayanan, Jian Hui Zhang. From laboratory Microgrid to real markets—challenges and opportunities. In: Proceedings of the 2011 IEEE 8th international conference on power electronics ECCE Asia ICPE ECCE; 2011. p. 264–71.

Ustun TS, Zayegh A, Ozansoy C. Electric vehicle potential in Australia: its impact on smartgrids. Ind Electron Mag IEEE 2013;7(4):15–25.

Weitemeyer S, Kleinhans D, Vogt T, Agert C. Integration of renewable energy sources in future power systems: the role of storage,”. Renew Energy 2015;75(0):14–20.

Zakeri B, Syri S. Electrical energy storage systems: a comparative life cycle cost analysis. Renew Sustain Energy Rev 2015;42(0):569–96.

Please cite this article as: Sbordone DA, et al. Reactive power control for an energy storage system: A real implementation in a Micro-Grid. Journal of Network and Computer Applications (2015), http://dx.doi.org/10.1016/j.jnca.2015.05.006